

AD-A214 559

RADC-TR-89-143
Final Technical Report
September 1989

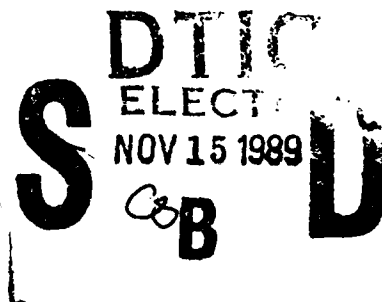


4

RAMAN SPECTROSCOPIC ANALYSIS OF IMPREGNATED CATHODES

University of Utah

S.B. Turcotte, J.R. Mitchell, R.E. Benner, R. W. Grow



APPROVED FOR PUBLIC RELEASE; DISTRIBUTION UNLIMITED.

ROME AIR DEVELOPMENT CENTER
Air Force Systems Command
Griffiss Air Force Base, NY 13441-5700

89 11 13 115

This report has been reviewed by the RADC Public Affairs Division (PA) and is releasable to the National Technical Information Service (NTIS). At NTIS it will be releasable to the general public, including foreign nations.

RADC-TR-89-143 has been reviewed and is approved for publication.

APPROVED:

Edward Daniszewski

EDWARD DANISZEWSKI
Project Engineer

APPROVED:

James W. Youngberg

JAMES W. YOUNGBERG, LtCol, USAF
Assistant Director of Surveillance

FOR THE COMMANDER:

John A. Ritz

JOHN A. RITZ
Directorate of Plans & Programs

If your address has changed or if you wish to be removed from the RADC mailing list, or if the addressee is no longer employed by your organization, please notify RADC (OCTP) Griffiss AFB NY 13441-5700. This will assist us in maintaining a current mailing list.

Do not return copies of this report unless contractual obligations or notices on a specific document require that it be returned.

UNCLASSIFIED

SECURITY CLASSIFICATION OF THIS PAGE

REPORT DOCUMENTATION PAGE				Form Approved OMB No. 0704-0188		
1a. REPORT SECURITY CLASSIFICATION UNCLASSIFIED			1b. RESTRICTIVE MARKINGS N/A			
2a. SECURITY CLASSIFICATION AUTHORITY N/A			3. DISTRIBUTION / AVAILABILITY OF REPORT Approved for public release; distribution unlimited.			
2b. DECLASSIFICATION / DOWNGRADING SCHEDULE N/A						
4. PERFORMING ORGANIZATION REPORT NUMBER(S) UTEC MD-89-017			5. MONITORING ORGANIZATION REPORT NUMBER(S) RADC-TR-89-143			
6a. NAME OF PERFORMING ORGANIZATION The University of Utah		6b. OFFICE SYMBOL (if applicable)	7a. NAME OF MONITORING ORGANIZATION Rome Air Development Center (OCTP)			
6c. ADDRESS (City, State, and ZIP Code) Department of Electrical Engineering 3280 Merrill Engineering Building Salt Lake City UT 84112			7b. ADDRESS (City, State, and ZIP Code) Griffiss AFB NY 13441-5700			
8a. NAME OF FUNDING / SPONSORING ORGANIZATION AFOSR		8b. OFFICE SYMBOL (if applicable) NE	9. PROCUREMENT INSTRUMENT IDENTIFICATION NUMBER F30602-84-C-0153			
8c. ADDRESS (City, State, and ZIP Code) Bolling AFB Wash DC 20332			10. SOURCE OF FUNDING NUMBERS			
			PROGRAM ELEMENT NO 61102F	PROJECT NO 2305	TASK NO J9	WORK UNIT ACCESSION NO 17
11. TITLE (Include Security Classification) RAMAN SPECTROSCOPIC ANALYSIS OF IMPREGNATED CATHODES						
12. PERSONAL AUTHOR(S) S. B. Turcotte, J. R. Mitchell, R. E. Benner, R. W. Grow						
13a. TYPE OF REPORT Final		13b. TIME COVERED FROM Sep 86 TO Dec 88		14. DATE OF REPORT (Year, Month, Day) September 1989		
15. PAGE COUNT 40						
16. SUPPLEMENTARY NOTATION Research accomplished in conjunction with Air Force Thermionics Engineering Research Program (AFTER) MD-88-050.						
17. COSATI CODES			18. SUBJECT TERMS (Continue on reverse if necessary and identify by block number)			
FIELD	GROUP	SUB-GROUP	Thermionic Cathodes Raman Spectroscopy			
09	01					
19. ABSTRACT (Continue on reverse if necessary and identify by block number) Two optical detection systems were used to obtain Raman spectra from impregnant samples, tungsten pellets, and cathode surfaces. The advantages of each system are described and their use for cathode diagnostics are explored. The Raman spectra from various impregnant samples are given and preliminary data from tungsten pellets and cathodes at low pressure and at temperatures as high as 860C are presented.						
20. DISTRIBUTION / AVAILABILITY OF ABSTRACT <input checked="" type="checkbox"/> UNCLASSIFIED/UNLIMITED <input type="checkbox"/> SAME AS RPT <input type="checkbox"/> DTIC USERS			21. ABSTRACT SECURITY CLASSIFICATION UNCLASSIFIED			
22a. NAME OF RESPONSIBLE INDIVIDUAL Edward Daniszewski			22b. TELEPHONE (Include Area Code) (315) 330-4381		22c. OFFICE SYMBOL RADC (OCTP)	

DD Form 1473, JUN 86

Previous editions are obsolete.

SECURITY CLASSIFICATION OF THIS PAGE

UNCLASSIFIED

UNCLASSIFIED

UNCLASSIFIED

ACKNOWLEDGMENT

We thank the AFTER Program under Air Force Contract F30602-84-C-0153 and the Free Electron Laser Biomedical Materials Science Program under Office of Naval Research contracts N00014-86-K-0258 and N00014-86-K-0710 for support of this work. We also thank Dr. Wayne Ohlinger of Semicon Associates for supplying the impregnant reference materials.

Accession For	
NTIS GRA&I	<input checked="" type="checkbox"/>
DTIC TAB	<input type="checkbox"/>
Unannounced	<input type="checkbox"/>
Justification	
By	
Distribution/	
Availability Codes	
Dist	Avail and/or Special
A-1	



TABLE OF CONTENTS

	<u>Page</u>
ACKNOWLEDGMENT	iii
LIST OF ILLUSTRATIONS AND TABLE	v
I. INTRODUCTION	1
II. INSTRUMENTATION	3
III. TEST VEHICLE	9
IV. IMPREGNANT MATERIAL SPECTRA	11
V. TUNGSTEN OXIDATION	15
VI. CATHODE SPECTRA	18
VII. DISCUSSION	28
REFERENCES	30

LIST OF ILLUSTRATIONS AND TABLES

<u>Figure</u>		<u>Page</u>
1	Optical multichannel apparatus (OMA) consisting of a triple spectrograph and liquid nitrogen cooled CCD detector used for the collection of Raman data	4
2	Comparison of the Raman spectra of WO_3 obtained in 0.1 second with the optical multichannel apparatus (bottom) and obtained in 15 minutes with a scanning spectrometer and photomultiplier (top)	6
3	Spatially resolved Raman data from a mixture of $BaCO_3$ and $BaWO_4$	8
4	Spatially resolved Raman data from a new 5-3-2 cathode surface	9
5	Diagram of test vehicle used for completion of optical measurements on cathodes at low pressure and high temperature	10
6	Raman spectra from impregnant sample Nos. 1 and 2	12
7	Raman spectra from impregnant sample Nos. 3, 4, and 5	13
8	Raman spectrum of a tungsten pellet that was heated at $600^\circ C$ for 3 hours and observed at room temperature	16
9	Temperature dependence of the measured Raman spectra from a tungsten pellet in a vacuum	17
10	Raman spectra from the surfaces of 5-3-2 and 4-1-1 cathodes compared to the spectra of impregnant sample Nos. 1 and 3 listed in Table 1	19
11	Raman spectra from three different positions on the surface of a 5-3-2 cathode	20
12	Raman spectrum of a 5-3-2 cathode (position No. 1 in Fig. 11) compared to the spectrum of barium tungstate	21
13	Spatially resolved Raman data from a temperature processed cathode at room temperature. The spatial extent of the cathode position axis is 0.5 mm	23
14	Comparison of processed cathode Raman spectrum with Raman spectra of WO_3 and BaO	24

Figure

Page

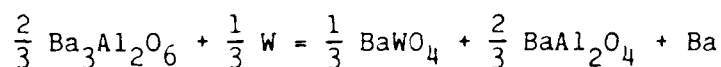
15	Temperature dependence of the measured Raman spectra from the processed cathode	26
----	----------------------------------------------------------------------------------------------	----

Table

1	Composition of impregnant samples	11
---	---------------------------------------------	----

I. INTRODUCTION

In 1957, Rittner et al.¹ developed a working model for the emission and evaporation characteristics of the impregnated cathode. Based on experimental work, they deduced that the impregnant material flows through the porous tungsten by Knudsen flow. On the cathode surface, barium is liberated by the reaction:



During the past 30 years, many investigators have worked to confirm the hypotheses made by Rittner et al. Various techniques have been used to detect the presence of barium on the tungsten surface and correlate evaporation rates with cathode lifetime. Auger electron spectroscopy was used by Springer et al.² to monitor barium and oxygen concentrations on the cathode surface. A direct correlation was found between Ba and O concentrations and optimal cathode operations. Haas et al.³ have used the scanning low-energy electron probe (SLEEP) technique to measure the work-function variation on the cathode surface. Through their work, a better understanding of the role of the BaO monolayers on the cathode surface was gained.

An extensive study on the thermochemistry of impregnant materials has been conducted by Hill et al.⁴ Using differential thermal analysis in conjunction with X-ray diffraction and scanning electron microscopy, they were able to elucidate the phase equilibria of the BaO-CaO-Al₂O₃ system in the high-baria region of the characteristic phase diagram.

Their studies make it possible to choose impregnant compositions in which the phases are known during both impregnation and cathode operation.

The goal of our own research is to monitor the chemical reactions that take place on the cathode surface. Towards this end, we have employed the technique of Raman scattering. The primary advantage of this technique is that chemical compound concentrations can be detected at elevated temperatures. This report will describe the experimental apparatus we have used for this spectroscopic study, as well as our preliminary results.

II. INSTRUMENTATION

In our previous Raman spectroscopic work,³ a conventional scanning spectrometer and single-channel photomultiplier detector have been used. Because of the accurate calibration, high elastic light rejection, and high resolution capabilities of this system, it is ideal for use in obtaining reference spectra from chemical compounds. To obtain Raman spectra from a cathode surface, however, monolayer sensitivity is required. Because the conventional scanning system does not have this capability, a multichannel detection system has been employed. The multichannel system is described below.

The optical multichannel apparatus (OMA) used for collection of the Raman data in this report is diagrammed in Fig. 1. Light from an argon laser operating at a power level of approximately 600 mW and at a wavelength of either 488 nm or 514.5 nm is focused using the cylindrical lens L1 onto a sample surface to form a line of excitation radiation having dimensions of approximately 100 micrometers \times 2.5 mm. The angle of incidence is approximately 60 degrees. Raman scattered radiation is collected at $f/1.2$ by the lens L2 and imaged by the lens L3 at $f/7$ onto the entrance slit of a triple spectrograph (Spex 1877). The first two diffraction gratings in the spectrograph are ruled 1200 groove/mm gratings which operate in a subtractive dispersion mode to reduce the amount of radiation at the laser wavelength which enters the third spectrograph stage, which contains a 1200 line/mm ruled grating. Wavelength dispersed light at the exit plane of the spectrograph is detected with a 384 \times 576 pixel CCD array which is cooled by liquid nitrogen

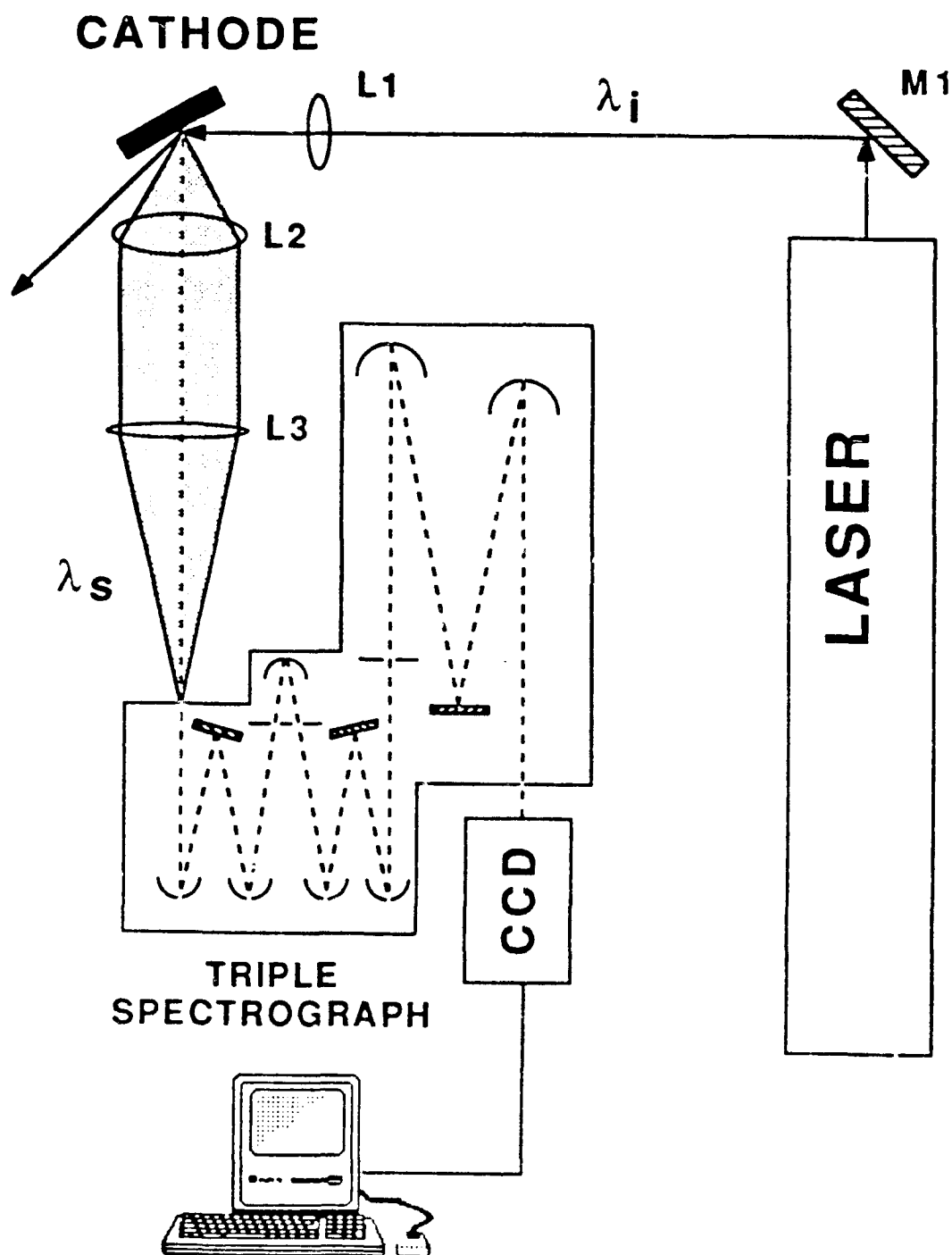


Fig. 1. Optical multichannel apparatus (OMA) consisting of a triple spectrograph and liquid nitrogen cooled CCD detector used for the collection of Raman data.

(Photometrics, Ltd.). Each pixel of the array is 23×23 micrometers in size. Using the 1200 groove/mm gratings and the array oriented with its 576 pixel axis along the direction of wavelength dispersion, the system is capable of simultaneously recording approximately 600 cm^{-1} of frequency-shifted Raman data. The shorter (384 pixel) axis of the array provides simultaneous spatial resolution of the Raman signals initiated by the excitation line on the sample.

Compared to the conventional scanning spectrometer, optical multi-channel detection offers several important advantages.⁶ The most obvious advantage arises from the parallel nature of the data collection process. Since over 500 channels of spectral data are recorded in parallel using the OMA, data acquisition is at least 500 times faster than with a single channel system assuming the quantum efficiencies of the two detectors are comparable. The quantum efficiency of our CCD detector (30-50 percent) is actually greater than that of the GaAs photomultiplier (~15 percent) used with the scanning spectrometer. Figure 2 compares Raman data obtained from WO_3 powder using the OMA and single channel systems. Consistent with the parallel advantage, the OMA data were recorded in a total time of 0.1 second compared to a time of approximately 15 minutes for the single channel system. Compared to the single channel results, the OMA data exhibit somewhat better resolution and similar signal-to-noise ratio. Tungsten oxide, however, has a large Raman cross section and is easily detected with either system. The OMA advantage becomes much more pronounced for the detection of extremely weak optical signals. When cooled to approximately -130°C , the CCD is capable of integrating signals for periods as long as an hour or more,

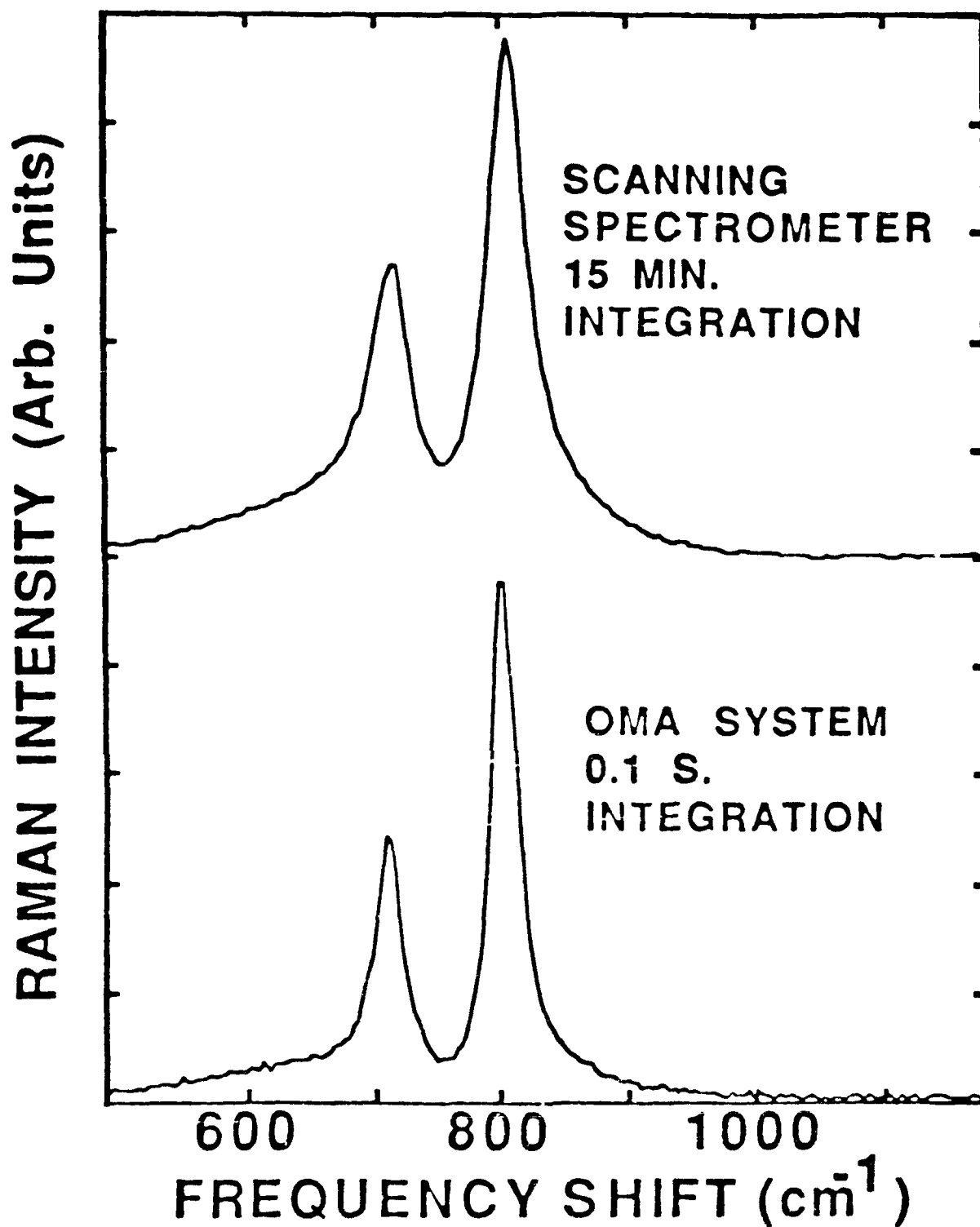


Fig. 2. Comparison of the Raman spectra of WO_3 obtained in 0.1 second with the optical multichannel apparatus (bottom) and obtained in 15 minutes with a scanning spectrometer and photomultiplier (top).

with extremely little accumulation of background noise beyond that which is present for integration periods as short as seconds. Using this mode of operation with the OMA, we have been able to obtain high quality spectra which could not be obtained at all using single channel detection.

An additional advantage of the OMA for cathode studies is the inherent spatial resolution which is afforded by the short axis of the array detector. Figure 3 is a photograph of the intensity distribution at the exit plane of the spectrograph as measured by the CCD and shown on a CRT display when a mixture of barium carbonate and barium tungstate powders was illuminated at the sample position. The first and fifth vertical lines are Raman peaks arising from barium carbonate, while the three central lines are Raman peaks from barium tungstate. The relative intensities along the vertical lines represent the relative amounts of the corresponding chemical compounds along the line of illumination. In regions where the barium tungstate peaks are bright, the barium carbonate peaks are dim. Since approximately 1 mm of sample dimension is imaged onto the 384 rows of vertical pixels, the chemical species present along the illuminated line of the sample are spatially resolved with an accuracy of a few micrometers.

The combined effects of high sensitivity and spatial resolution available with the OMA are illustrated in Fig. 4. This photograph was obtained in a manner similar to Fig. 3 by illuminating a new 5-3-2 cathode in air with a line of radiation at a wavelength of 488 nm. To obtain the data, a CCD integration time of 2 hours was employed. The relatively dim, nearly continuous, vertical line which appears at a

frequency shift of approximately 1060 cm^{-1} arises from a relatively uniform distribution of barium oxide along the illuminated line. The three peaks at lower frequency shift having a shorter extent in the vertical direction arise from an impurity on the cathode surface. Based on the size of these peaks in the vertical direction, we conclude that the impurity is approximately 150 micrometers in size. By comparing the spectral signature of the impurity along the frequency shift axis of the display with our collection of reference Raman spectra,⁵ we also conclude that the impurity consists of a mixture of tungsten oxide and tungstate. The horizontal lines in Fig. 4 are also of interest. They suggest the presence of a fluorescing species which is not uniformly distributed and might arise from the roughness of the cathode itself or from material contained within its pores.

III. TEST VEHICLE

Although Raman studies of new cathodes and reference compounds are of interest in establishing the capabilities of the Raman technique, they are not especially useful for probing cathode chemistry. Consequently, we have developed a test vehicle with adequate optical access for conducting Raman scattering studies of cathodes at low pressure and high temperature. Our test chamber is diagrammed in Fig. 5. A support structure for a cathode and heater is housed within several vacuum flanges, and a window is placed above the cathode for optical access. Vacuum feed-throughs are provided for electrical connections. For Raman measurements, a new cathode was installed in the chamber and evacuated to a pressure of 10^{-9} torr using a vacuum pumping station. The temperature of the cathode, monitored using an optical pyrometer, was then slowly increased to a maximum of 980°C with the vacuum maintained near 10^{-9} torr. After approximately 24 hours at 980°C , the cathode heater and vacuum pump were disconnected, and the sealed chamber was transported to the Raman system. During the acquisition of Raman data, a getter pump attached to the chamber maintained the vacuum near 10^{-9} torr.

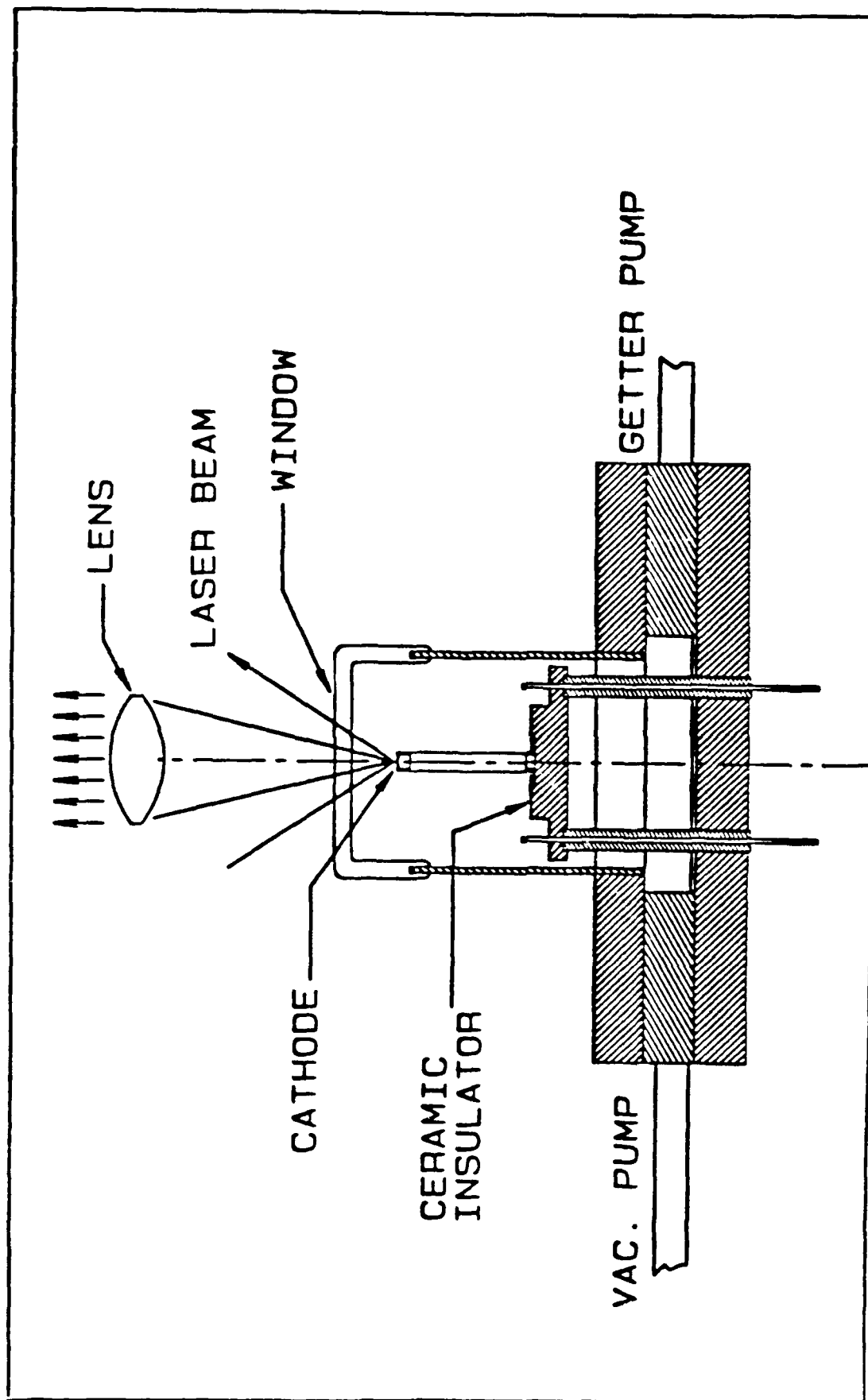


Fig. 5. Diagram of test vehicle used for completion of optical measurements on cathodes at low pressure and high temperature.

IV. IMPREGNANT MATERIAL SPECTRA

Powder samples with different molar ratios of BaO, CaO, and Al₂O₃ have been provided by Semicon Associates. The molar percents for the five powders and the phase of the BaO (abbreviated as B) and Al₂O₃ (abbreviated as A) compounds are shown in Table 1.

Table 1. Composition of impregnant samples.

Sample No.	Phase	Mole Percent		
		BaO	CaO	Al ₂ O ₃
1	B ₃ A	56.25	18.75	25
2	B ₃ A	71.0	4.0	25
3	B ₄ A	59.5	20.5	20
4	B ₄ A	74.5	5.5	20
5	B ₄ A	69.0	11.0	20

The impregnant samples were carefully packed by Semicon Associates to avoid contamination from the air. In a chamber with a controlled flow of N₂, the samples were removed from their packages and sealed in glass capillary tubes. The samples could then be mounted in place of the cathode in Fig. 1. With a laser excitation wavelength of 488 nm, the Raman spectra from these five samples were obtained using the scanning spectrometer. The results are shown in Figs. 6 and 7. Similar data were obtained with an excitation wavelength of 514 nm, confirming that the spectra arise from Raman peaks.

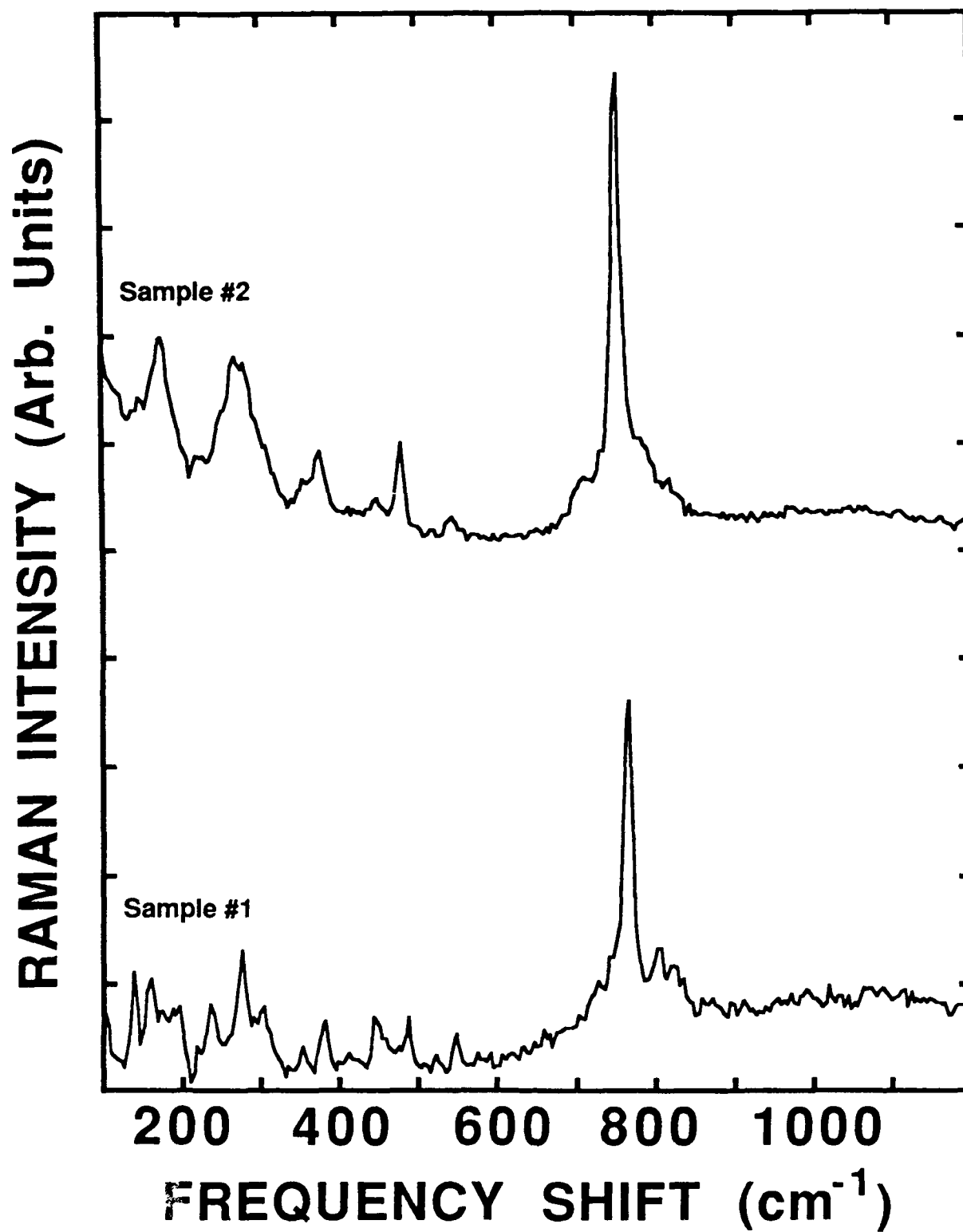


Fig. 6. Raman spectra from impregnant sample Nos. 1 and 2.

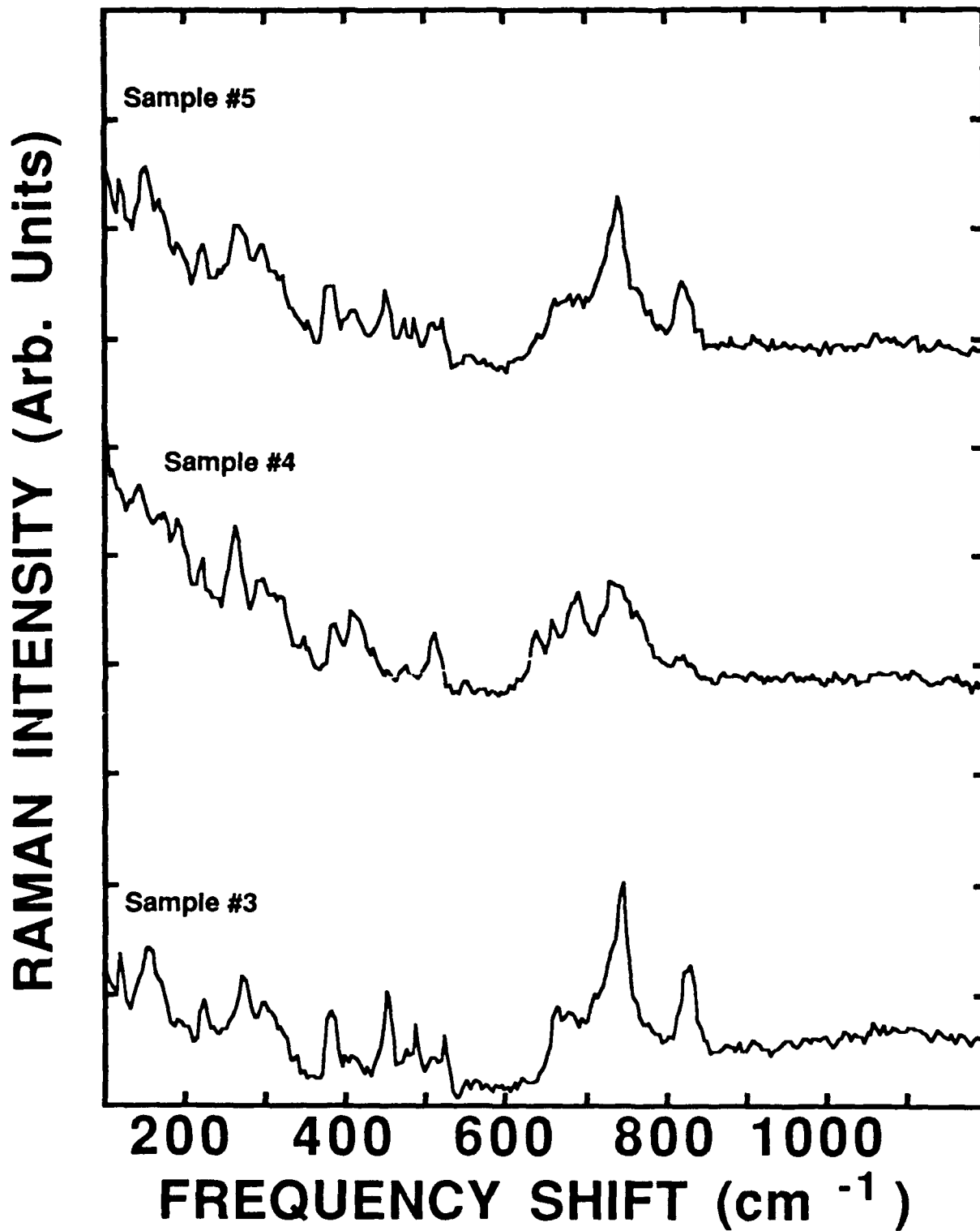


Fig. 7. Raman spectra from impregnant sample Nos. 3, 4, and 5.

In Figs. 6 and 7, variations are observed in the Raman spectra from the five impregnant samples. For example, the effect of changing the Al_2O_3 molar ratio is observed in comparing the spectra from sample Nos. 1 and 2 with those of sample Nos. 3, 4, and 5. The peak at approximately 750 cm^{-1} changes dramatically. The Raman peak at approximately 820 cm^{-1} in sample Nos. 1, 3, and 5 is absent in sample Nos. 2 and 4. This could be due to the relatively small molar percent of CaO found in sample Nos. 2 and 4.

V. TUNGSTEN OXIDATION

The oxidation of tungsten has been investigated by heating tungsten pellets to various temperatures in atmospheric conditions and then obtaining Raman spectra from the oxidized surface at room temperature. For example, Fig. 8 shows the Raman spectrum from a tungsten pellet that was heated at 600°C for 3 hours. The strong Raman peaks at approximately 127, 254, 702, and 802 cm^{-1} are the characteristic peaks of tungsten oxide.

A tungsten pellet with an oxidized surface has also been examined in a vacuum at elevated temperatures using the test vehicle shown in Fig. 5. A heater was mounted behind the tungsten pellet and the pellet was heated to approximate temperatures of 600°C and 850°C. A comparison of the spectra at three different temperatures is shown in Fig. 9. A broadening and slight shift of the Raman peak at approximately 820 cm^{-1} is observed as the temperature is increased.

The difference between the spectrum of the tungsten pellet in Fig. 9 at room temperature (25°C) and the spectrum of the pellet shown in Fig. 8 is to be noted. When the tungsten pellet was placed in the test vehicle with subsequent evacuation of the chamber, the yellow-green WO_3 powder (responsible for the spectrum in Fig. 8) was removed from the tungsten surface and only a blue-black adherent oxide remained. It is the spectrum of the blue-black adherent oxide that is being examined in Fig. 9.

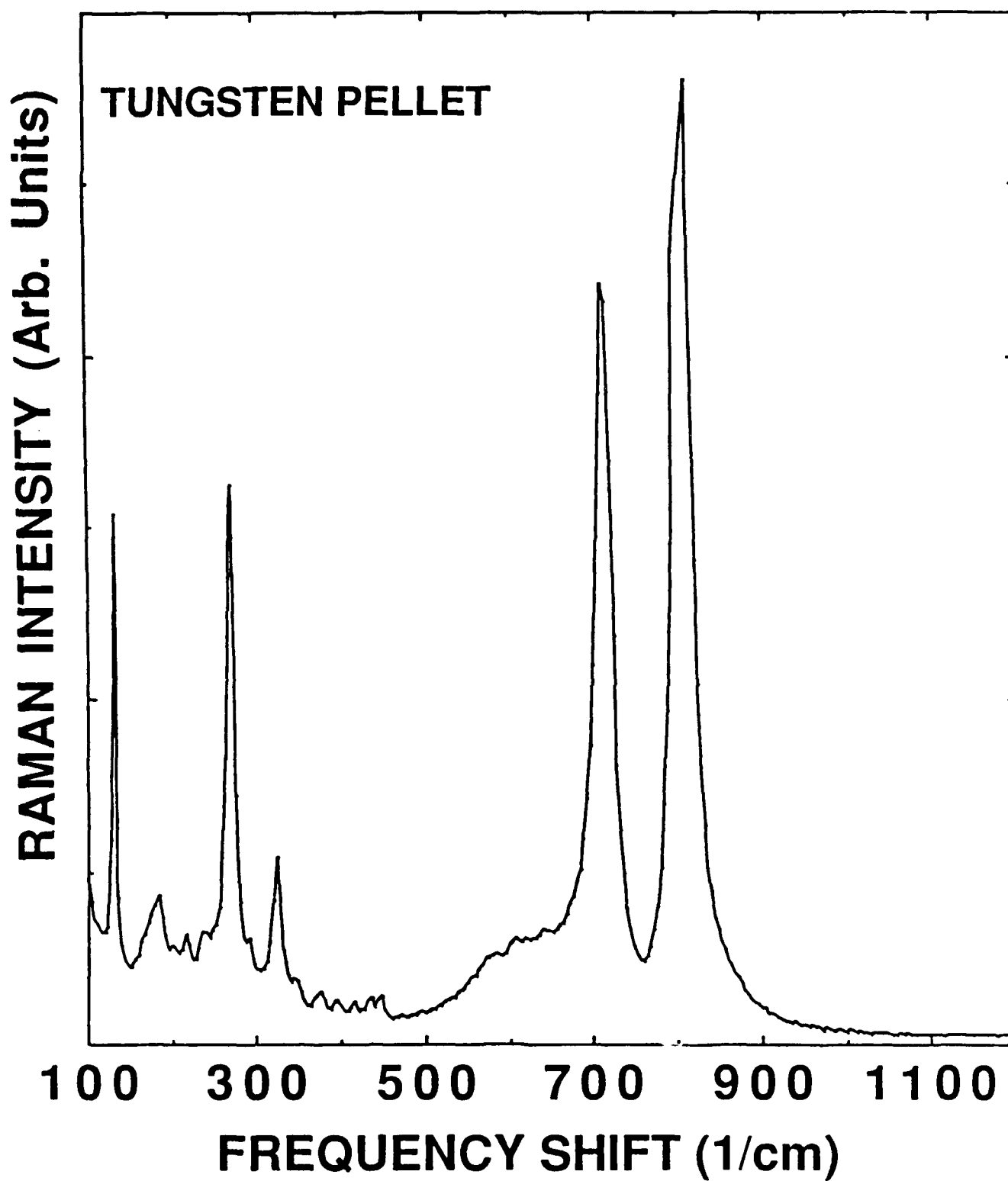


Fig. 8. Raman spectrum of a tungsten pellet that was heated at 600°C for 3 hours and observed at room temperature.

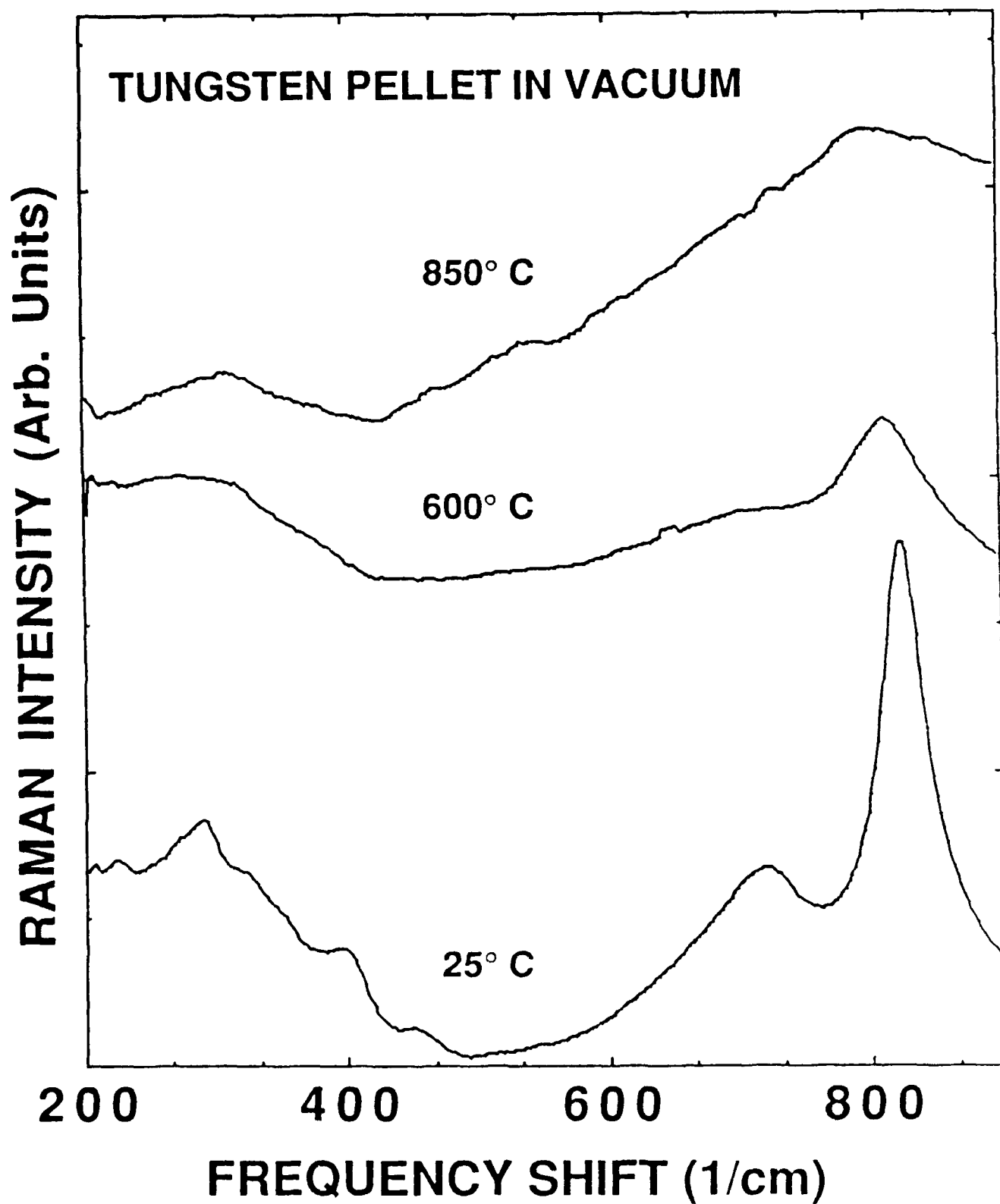


Fig. 4. Temperature dependence of the measured Raman spectra from a tungsten pellet in a vacuum.

VI. CATHODE SPECTRA

Raman spectra have been obtained from the surfaces of 5-3-2 and 4-1-1 cathodes. Initially, the cathodes studied were new and unprocessed. In Fig. 10, the Raman spectra of the 5-3-2 and 4-1-1 cathodes are compared to the Raman spectra of impregnant sample Nos. 1 and 3. A comparison of this kind could be used to determine the phase of the impregnant on the cathode surface and the extent to which it interacts with the tungsten.

The impregnated cathode surface consists of a porous tungsten matrix with impregnant material filling the pores. The average tungsten grain diameter is approximately 4.5 μm and the average pore diameter is approximately 3 μm . Our Raman microprobe system⁵ is capable of illuminating a sample area with a diameter of approximately 2 μm . Therefore, our system can be used to examine the inhomogeneity on the cathode surface.

Figure 11 shows Raman spectra from three different positions on the 5-3-2 cathode surface. A comparison of the spectra at these three positions to the spectra from our reference compounds and our impregnant samples suggest the following conclusions:

1. Position No. 1 corresponds to the interface between the tungsten grain and the impregnant material. From a comparison of the spectrum at Position No. 1 of the 5-3-2 cathode with the spectrum of barium tungstate (see Fig. 12), it is probable that barium tungstate forms at the interface.

RAMAN INTENSITY (Arb. Units)

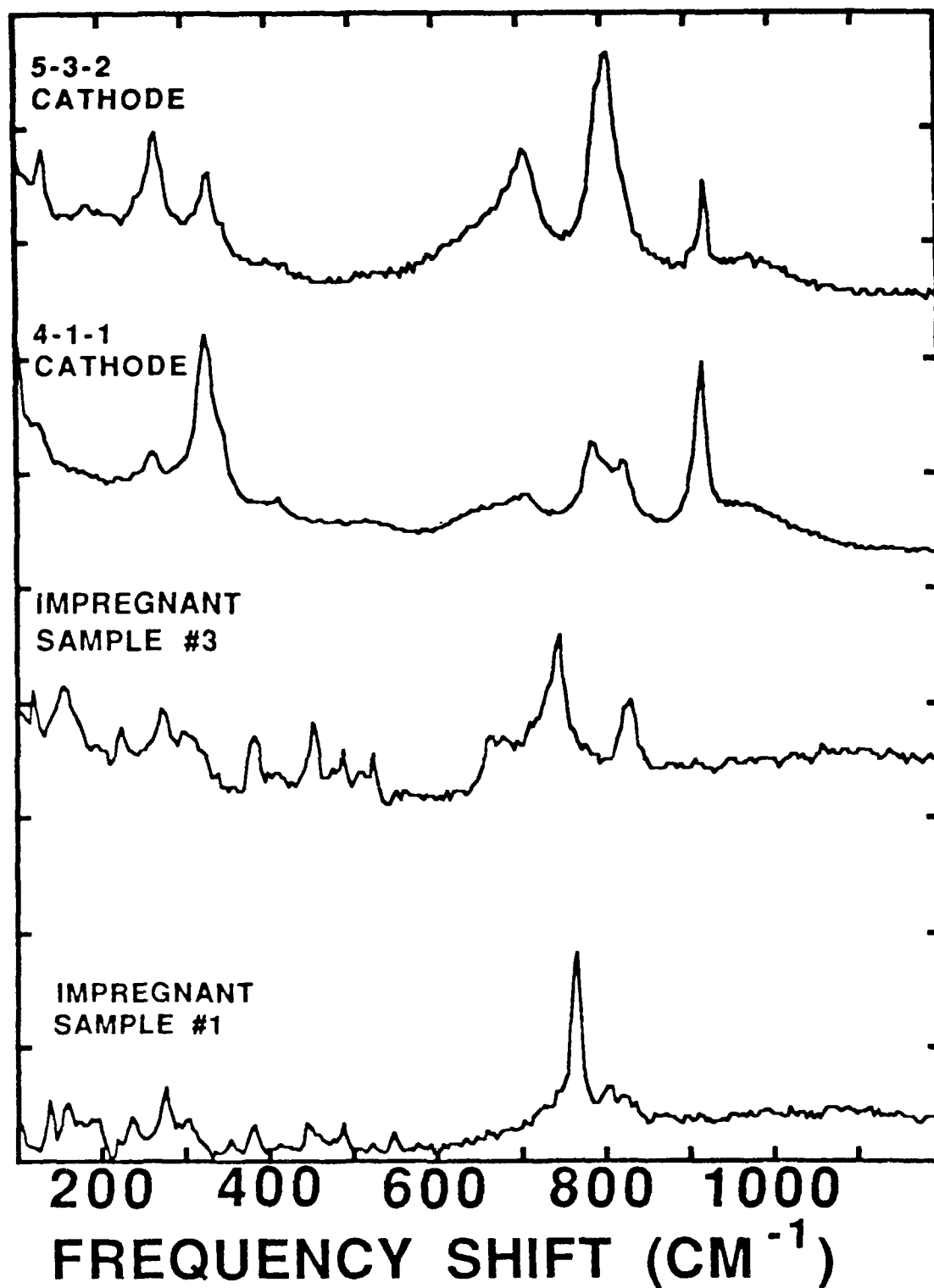


Fig. 10. Raman spectra from the surfaces of 5-3-2 and 4-1-1 cathodes compared to the spectra of impregnant sample Nos. 1 and 3 listed in Table 1.

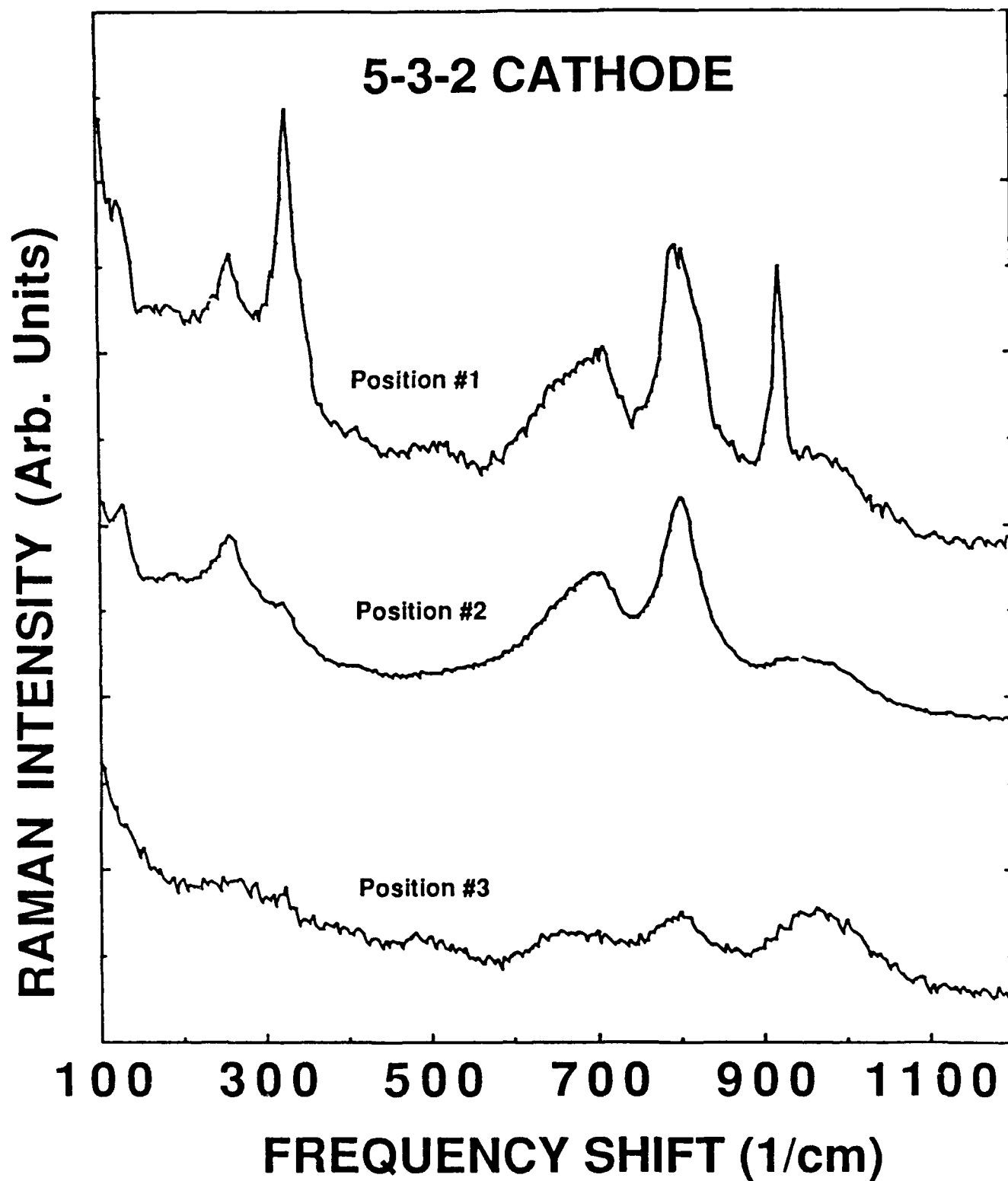


Fig. 11. Raman spectra from three different positions on the surface of a 5-3-2 cathode.

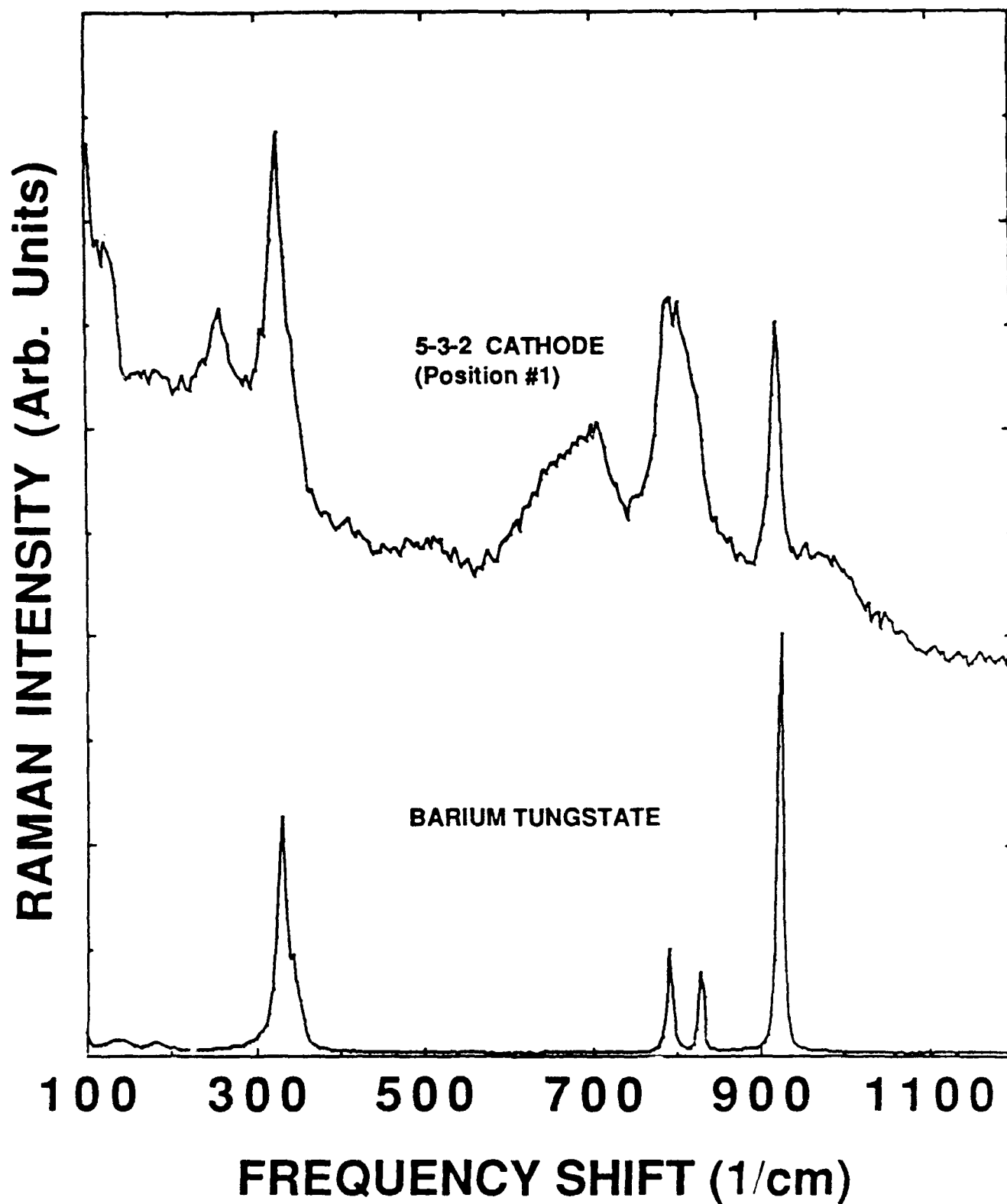


Fig. 12. Raman spectrum of a 5-3-2 cathode (position No. 1 in Fig. 11) compared to the spectrum of barium tungstate.

2. Position No. 2 represents a sampling of the impregnant material in the pores. The strong peaks at 700 cm^{-1} and 800 cm^{-1} are characteristic of the spectra from the impregnant samples shown in Figs. 6 and 7.
3. Position No. 3 is representative of the spectra from a tungsten grain, since metallic tungsten does not exhibit any Raman peaks.

After processing the cathode at high temperature in vacuum, spatially resolved Raman data similar to Fig. 4 were obtained at room temperature. Rather than displaying the results in photograph form, we plotted the digitized intensity values from a portion of the CCD array in a three-dimensional representation shown in Fig. 13. With excitation at 514.5 nm , a relatively strong Raman peak is observed at a frequency shift of 813 cm^{-1} , and two smaller Raman peaks at frequency shifts at 706 cm^{-1} and 673 cm^{-1} are just barely detected. The spatial extent along the cathode position axis is approximately 0.5 mm , which corresponds to 25 micrometers per spectrum. To improve the signal-to-noise ratio of the plotted data, the intensity values from groups of adjacent vertical pixels were averaged with some sacrifice in spatial resolution. Nevertheless, the data of Fig. 13 suggest a relatively uniform distribution of chemical species across the cathode surface. Better signal-to-noise ratios can be obtained by averaging nearly all of the pixels along the vertical axis of the array to obtain a single averaged Raman spectrum for the cathode. Results of this type are shown in Fig. 14. The Raman spectrum for the processed cathode in this figure extends over a broader range of frequency shift than in Fig. 13 simply because

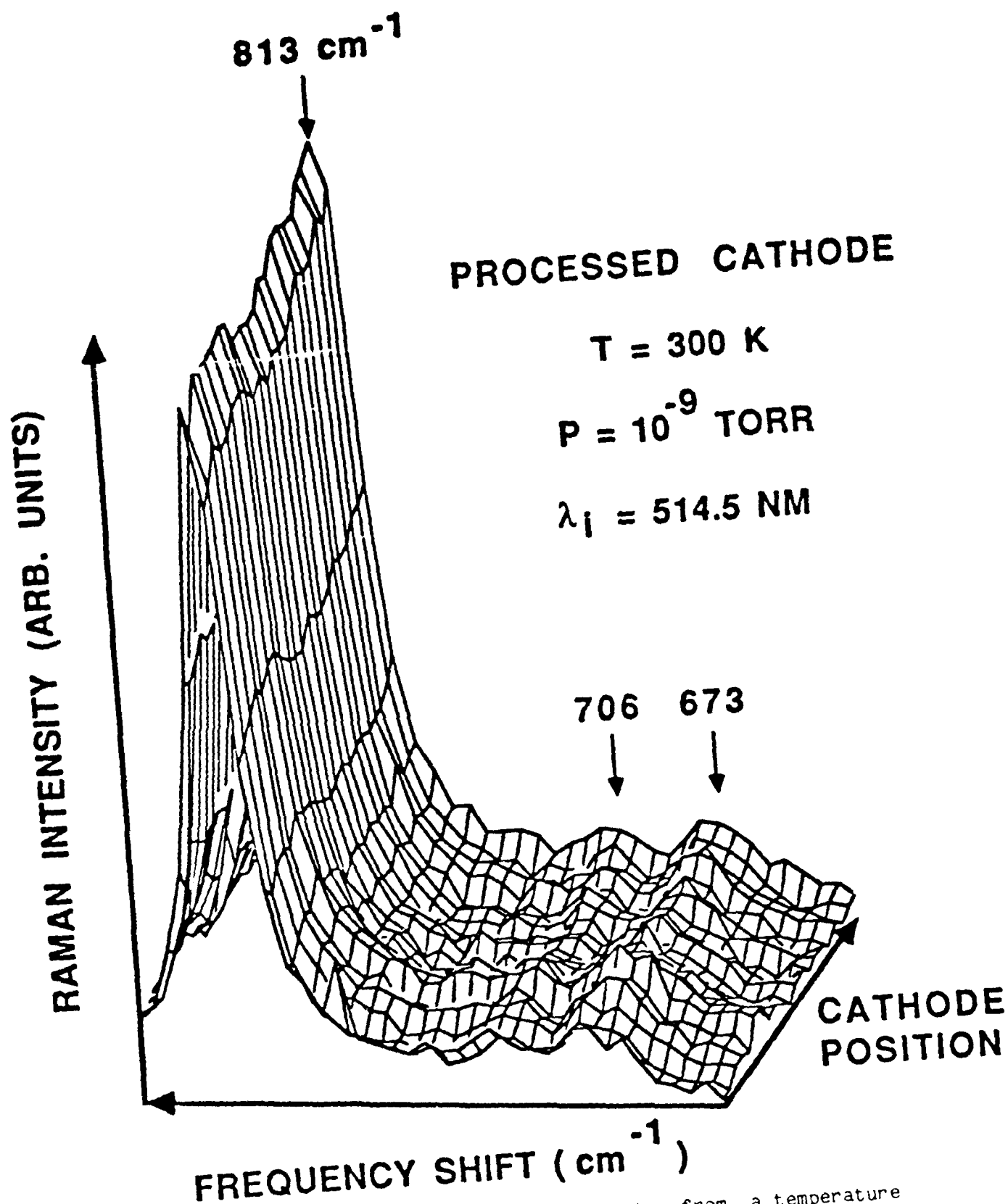


Fig. 13. Spatially resolved Raman data from a temperature processed cathode at room temperature. The spatial extent of the cathode position axis is 0.5 mm.

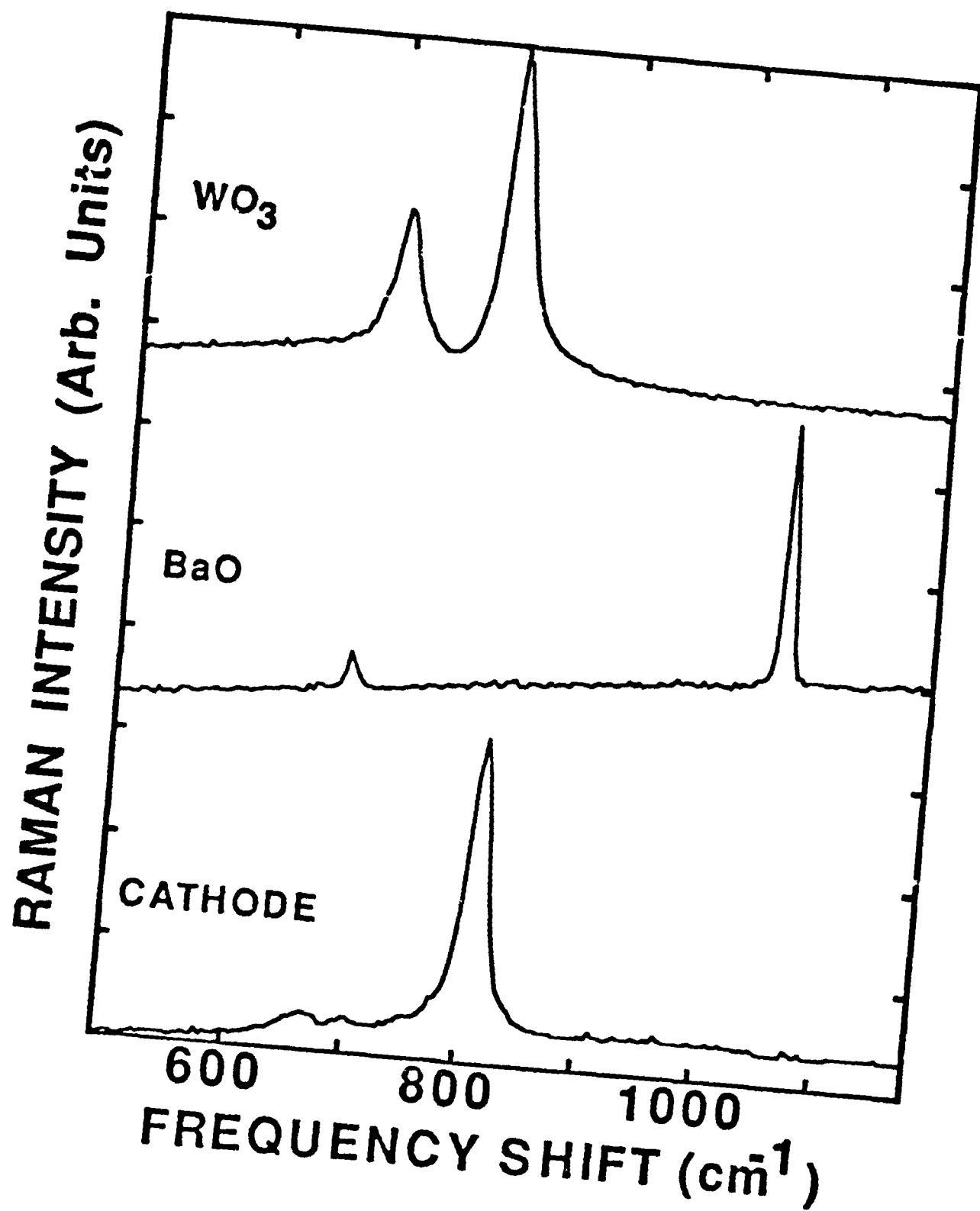


Fig. 14. Comparison of processed cathode Raman spectrum with Raman spectra of WO₃ and BaO.

more horizontal pixels were used in preparing the plot. After averaging, the Raman peaks at 673 cm^{-1} and 706 cm^{-1} become much better resolved. In contrast to the data of Fig. 13 which were recorded using an incident wavelength of 514.5 nm , the data of Fig. 14 were recorded using an incident wavelength of 488 nm . The incident wavelength was changed to ensure that the peaks appearing in the cathode spectrum were frequency-shifted Raman peaks rather than non-Raman peaks appearing at a fixed wavelength. The processed cathode Raman spectrum is also compared in Fig. 14 with reference spectra obtained with the OMA for BaO and WO_3 . Surprisingly, there is no indication of BaO in the cathode spectrum.

A comparison of the Raman spectra of the cathodes in Figs. 11 and 14 illustrate the effects of processing. The impregnant material has evaporated from the cathode surface and an oxide has been formed. The surfaces of cathodes with various operational lifetimes have also been analyzed. In all cases, there is an absence of the characteristic Raman peaks of the barium tungstate and impregnant found on the unprocessed cathode.

Raman spectra of the processed cathode were obtained as a function of temperature. Results obtained with an excitation wavelength of 488 nm for temperatures between 25°C and 860°C are shown in Fig. 15. The spectrum for 25°C is the same as that plotted in Fig. 14. With increasing temperature, the Raman peak at 813 cm^{-1} broadens and becomes more difficult to observe. The rising background toward higher frequency shift at the highest temperatures arises from the presence of blackbody radiation, which interferes with detection of the Raman spectrum of the

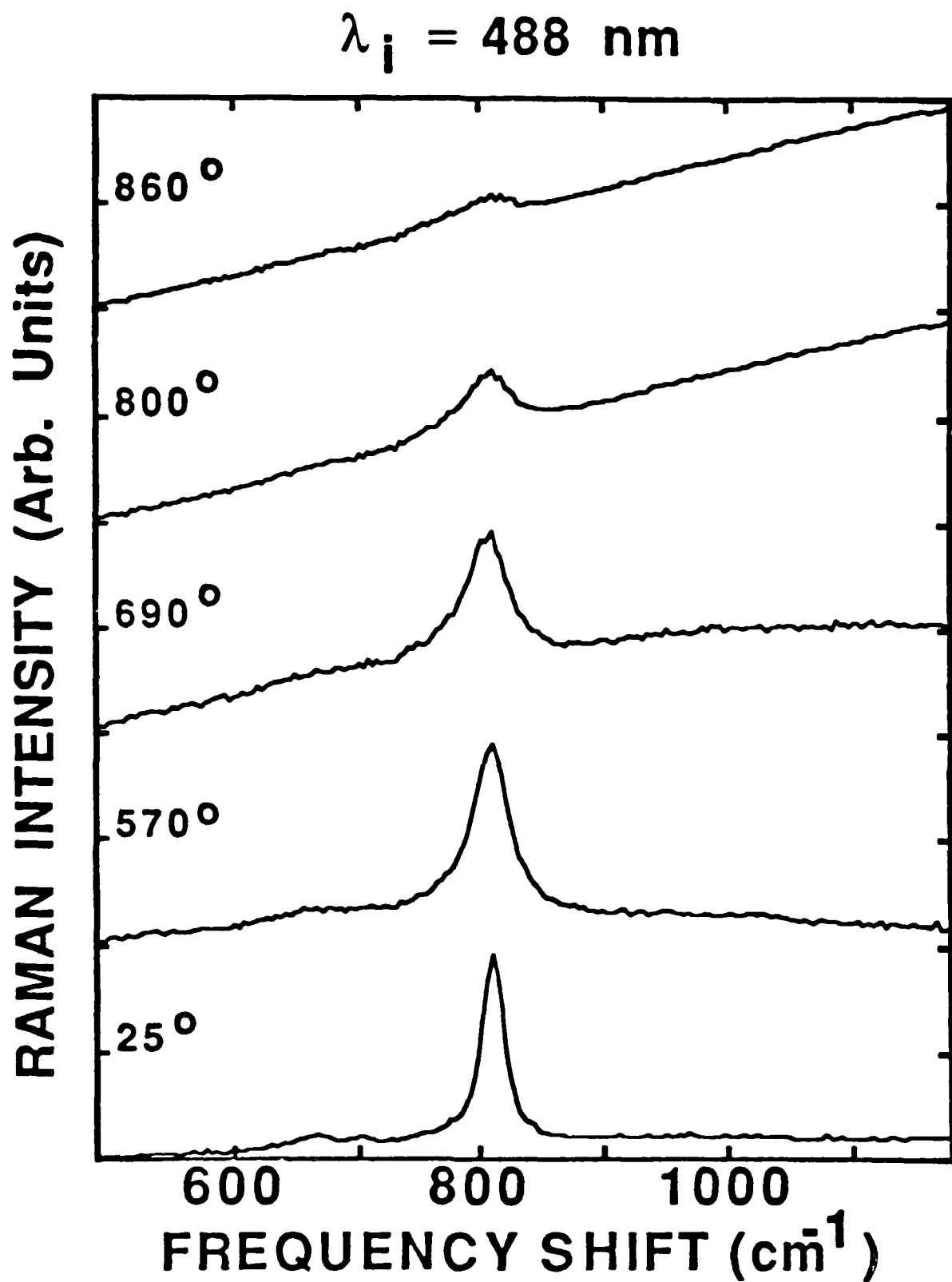


Fig. 15. Temperature dependence of the measured Raman spectra from the processed cathode.

cathode surface. Nevertheless, the Raman data indicate that the chemical composition of the cathode surface remains constant over the range of temperatures investigated.

VII. DISCUSSION

The optical multichannel apparatus and test vehicle have allowed us to further our Raman spectroscopic analysis of cathode surfaces. The spectra from processed and unprocessed cathodes have been compared to the spectra from impregnant mixtures, oxidized tungsten pellets, and reference compounds.

The success of this preliminary work suggests the feasibility of conducting a series of chemical studies beginning with impregnant samples and leading to chemical analysis of operating cathodes. With the impregnant samples mounted in the test vehicle, we can begin to examine the Raman spectra as a function of temperature. In general, the Raman peaks associated with the different samples can be expected to broaden with increasing temperature, and some of the compounds are likely to undergo phase changes which could significantly alter their spectra. Collection of a library of spectra as a function of temperature will aid in later interpretations of spectra associated with chemical reaction products, as well as provide a means of optimizing the high temperature capability of the Raman apparatus.

Our progression of chemical studies can include optical examinations of chemical reactions which occur when mixtures of elements and compounds are heated on a tungsten substrate. To accomplish this, a tungsten foil can be mounted in the evacuated test vehicle. The Raman spectra and emission characteristics can then be obtained with controlled fluxes of oxygen, barium, and calcium admitted into the test vehicle. Polarized Raman measurements can be made by varying the input

laser polarization and the position and direction of an analyzer placed in the scattered beam. The selection rules that govern Raman emission from molecules can be used to determine the orientation and nature of the barium and oxygen bonds on the tungsten surface. Different spectra will result depending on the intermolecular adhesive forces and also the coordination that exists between the atoms. Tungsten oxidation and poisoning mechanisms can be explored through these experiments.

REFERENCES

1. E. S. Rittner, W. C. Rutledge, and R. H. Ahlert, "On the Mechanism of Operation of the Barium Aluminate Impregnated Cathode," Journal of Applied Physics, Vol. 28, No. 12, December 1957, pp. 1468-1473.
2. R. W. Springer and T. W. Haas, "Auger Electron Spectroscopy Study of Cathode Surfaces During Activation and Poisoning," Journal of Applied Physics, Vol. 45, No. 12, December 1974, pp. 5260-5263.
3. G. A. Haas, H. F. Gray, and R. E. Thomas, "Effects of S, Ba, and C on Impregnated Cathode Surfaces," Journal of Applied Physics, Vol. 46, No. 8, August 1975, pp. 3293-3301.
4. D. N. Hill, R. E. Hann, and P. R. Switch, "Thermochemistry of Dispenser Cathode Impregnant Materials: Phase Equilibria in the BaO-CaO-Al₂O₃ System," RADC-TR-87-54 Final Technical Report, August 1987.
5. R. E. Benner, J. R. Mitchell, and R. W. Grow, "Raman Scattering as a Diagnostic Technique for Cathode Characterization," Technical Report AFTER-23, Rome Air Development Center Contract F30602-82-C-0161, December 29, 1986.
6. C. A. Murray and S. B. Dierker, "Use of an Unintensified Charge-Coupled Device Detector for Low Light-Level Raman Spectroscopy," Journal of the Optical Society of America, Vol. 3, No. 12, December 1986, pp. 2151-2159.



MISSION of Rome Air Development Center

RADC plans and executes research, development, test and selected acquisition programs in support of Command, Control, Communications and Intelligence (C³I) activities. Technical and engineering support within areas of competence is provided to ESD Program Offices (POs) and other ESD elements to perform effective acquisition of C³I systems. The areas of technical competence include communications, command and control, battle management information processing, surveillance sensors, intelligence data collection and handling, solid state sciences, electromagnetics, and propagation, and electronic reliability/maintainability and compatibility.